Dynamic hand proprioception via a wearable glove with fabric sensors

Lily Behnke¹, Lina Sanchez-Botero¹, William R. Johnson III¹, Anjali Agrawala¹, and Rebecca Kramer-Bottiglio¹

Abstract—Continuous enhancement in wearable technologies has led to several innovations in the healthcare, virtual reality, and robotics sectors. One form of wearable technology is wearable sensors for kinematic measurements of human motion. However, measuring the kinematics of human movement is a challenging problem as wearable sensors need to conform to complex curvatures and deform without limiting the user's natural range of motion. In fine motor activities, such challenges are further exacerbated by the dense packing of several joints, coupled joint motions, and relatively small deformations. This work presents the design, fabrication, and characterization of a thin, breathable sensing glove capable of reconstructing fine motor kinematics. The fabric glove features capacitive sensors made from layers of conductive and dielectric fabrics, culminating in a non-bulky and discrete glove design. This study demonstrates that the glove can reconstruct the joint angles of the wearer with a root mean square error of 7.2 degrees, indicating promising applicability to dynamic pose reconstruction for wearable technology and robot teleoperation.

I. INTRODUCTION

Wearable systems invite tangible interactions with robots in contexts such as virtual reality (VR), augmented reality (AR), and teleoperation [1]–[3]. Recent developments in wearable technology have incorporated soft sensing mechanisms for kinematic measurements [4], [5]. However, human motion invokes challenges associated with complex curvatures and form factors to which rigid systems do not comply. Soft sensors present a promising solution for the challenges associated with measuring human kinematics due to their deformability and robustness under strain [6], [7]. Notwithstanding the advantages of soft sensors, fine motor joints present unique challenges for kinematic estimation due to their small angular displacements, coupled joint motions, and number of joints in close proximity.

Many sensing gloves have been designed for applications ranging from VR to robotics [8]–[19]; however, current solutions include bulky mechanical components and complex wiring systems that impede motion and cause discomfort [9]–[11]. Other gloves include elastomer-based sensors that prevent the overall breathability and washability of the glove [15]–[19]. Here, we present a wearable sensing glove made entirely of fabrics to minimize the amount of material

*This work was supported by a NSF grant no. IIS-1954591. The study received IRB approval (Protocol ID 2000031654, approved by the Human Investigation Committee 2B with the Yale Human Research Protection Program)

¹School of Engineering and Applied Sciences, Yale University, New Haven, CT, USA email:{lily.behnke, lina.sanchez-botero, will.johnson, anjali.agrawala,rebecca.kramer}@yale.edu

required for sensing, while maintaining properties traditional to garments.

Fabric-based electronics allow the tight coupling of technology into traditional garments [20]–[22]. We previously introduced fabric-based strain sensors that can be easily integrated into garments while maintaining properties native to fabrics, including breathability and washability [23]. While fabric-based technologies have been implemented toward fine motor motion monitoring, limitations in fabric-based sensing gloves still remain with respect to the quantification of accuracy, minimalistic design, and the conservation of properties inherent to textiles [12]–[14].

This work adapts our previously developed fabric sensor to measure the fine motions of the hands. We detail the fabrication process of a fabric sensing glove and demonstrate the glove's ability to accurately estimate joint angles compared to ground truth from a motion capture system. The use of the fabric sensor in the form of a glove improves upon current solutions that include bulky, cumbersome, and uncomfortable components. This work seeks to demonstrate the manufacturing and quantified accuracy of a fully fabric sensing glove toward dynamic hand proprioception.

II. DESIGN AND FABRICATION

A. Capacitive Strain Sensors

We previously introduced a fabric capacitive strain sensor for integration with commercially available garments for gross motor motion monitoring [23]. This sensor is made from multiple layers of conductive fabric (76% Nylon and 24% elastic fiber, Less EMF Inc. Cat. #A321) separated by dielectric layers (Nylon 4-way stretch fabric, 80% Nylon and 20% Spandex), which are adhered to each other with a breathable thermoplastic adhesive film (Bemis Associates, Inc.). Full fabrication details can be found in our previous work [23]. The mechanics of the sensor are modeled after an ideal parallel plate capacitor.

$$C = \varepsilon \varepsilon_0 \frac{A}{d}$$

As the sensor is stretched, the overlapping area between the conductive electrodes increases and the dielectric thickness decreases, thereby increasing the sensor's capacitance.

B. Glove Fabrication

The design and fabrication of the glove are shown in Figure 1. Ten capacitive fabric sensors capture the motion of the metacarpophalangeal (MCP) and proximal interphalangeal (PIP) joints of each finger. The distal interphalangeal (DIP)

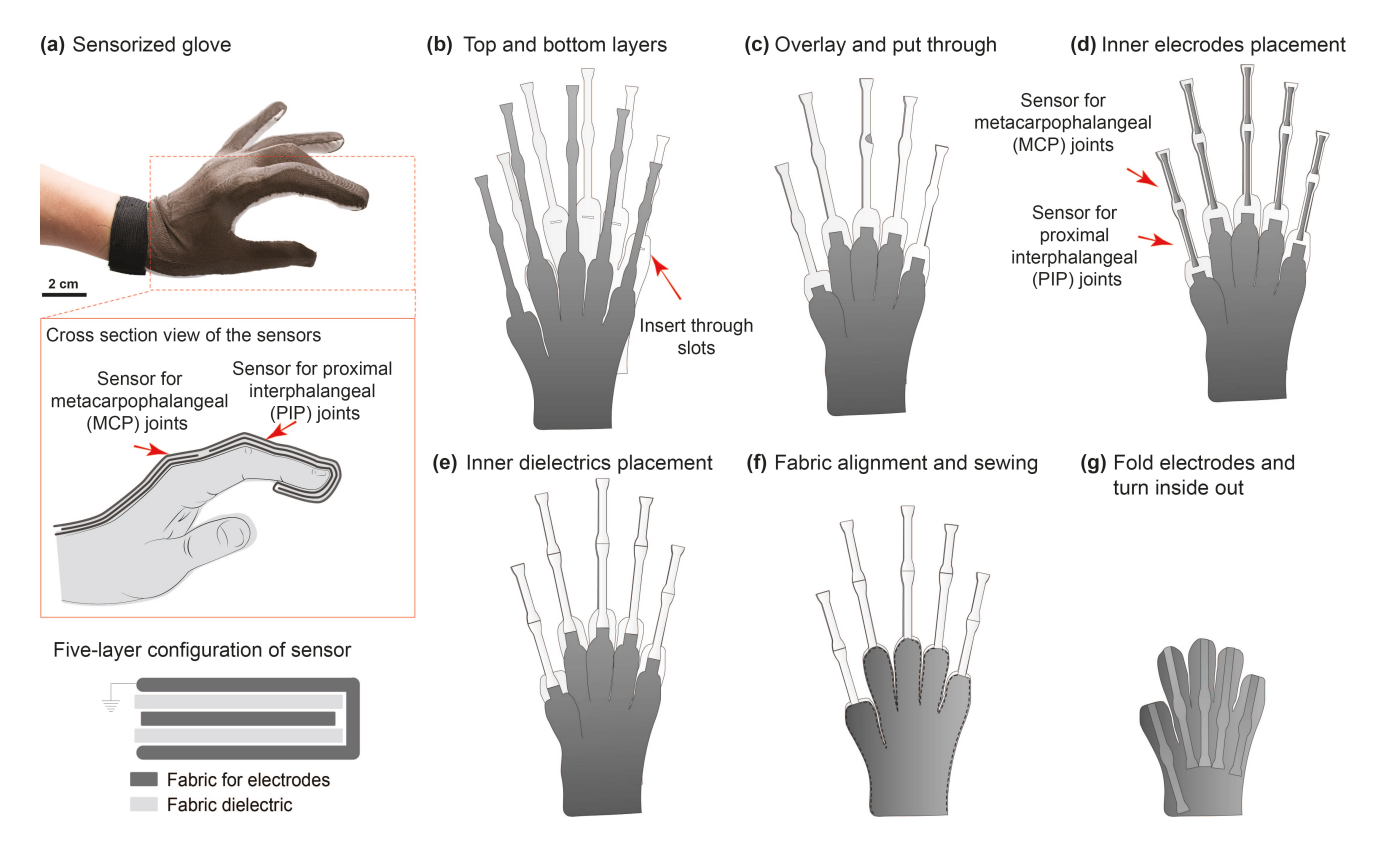


Fig. 1. (a) Photograph of the sensorized glove with the capacitive sensors along the middle phalanges of each finger to capture the movement of the metacarpophalangeal and proximal interphalangeal joints. Inset shows a close-up schematic of the cross-section of the sensors in the 5-layer capacitive sensor configuration. Fabrication steps of the sensorized glove (b) Top layer (common ground) and bottom layer of the glove were laser cut into desired shapes. (c) The extended shapes of the top layer were inserted through the cutouts of the bottom layer. (d) Placement of inner electrodes to sense the movement of both the metacarpophalangeal and proximal interphalangeal joints. (e) Second dielectric layer overlay. (f) Alignment and sewing of the top and bottom hand silhouettes. (g) Electrodes were folded to complete the 5-layer configuration of the capacitive sensor. The glove was turned inside out, and an elastic wristband was sewn on (see photograph in (a)). Capacitive sensor values were digitized using an MPR121 connected to an Arduino Uno.

joint is excluded since its motion is coupled to the motion of the PIP joint and it possesses a limited range of motion [24]. Each sensor is directly integrated into the garment rather than sewn into a commercially available glove. The entire top layer of the glove acts as a common electrical ground for all of the sensors, and the bottom layer serves as one of the two dielectric layers within each sensor, as shown in Figure 1a. The sensors reside on the underside of the glove's top layer, which, when worn, allows each sensor to rest directly on top of the finger. By fabricating the sensors as a part of the garment itself rather than attaching them onto one, we minimize the amount of material added, improving comfort and reducing any mechanical restriction of finger motion.

The layout of the sensors with respect to a single finger is shown in Figure 1a. The sensors were sized to each finger joint in order to accurately capture its motion. To fabricate the glove, the top outer electrode layer and bottom dielectric layers were laser cut first, then the top layer of the glove was looped through the bottom patterned layer of the glove to act as the common ground and first dielectric layer of each sensor (Figure 1b-c). Next, the remaining inner electrode and dielectric layers of each sensor were added to the existing base ground and dielectric (Figure 1d-e). The breathable adhesive and a heat press were used to adhere all the layers

together at 160°C. The glove was then sewn together and the sensors were folded over and adhered to complete the five layer configuration (Figure 1f-g). Wire leads were attached to each electrode within the glove, and one more was connected to the base of the top layer, which is the common ground. These leads were sewn to the base of the glove closest to the wrist so as to not interfere with motion. Following the fabrication of the glove, a cuff was sewn onto the wrist of the glove with a Velcro fastener (Figure 1a). This cuff acts as a stabilization mechanism to prevent shifting and slipping of the glove during motion.

III. UNIT CHARACTERIZATION

To investigate the response of the sensor, electromechanical characterization of the unit was performed both in free space and with on-hand boundary conditions. The free space characterization of the sensor was performed via a uniaxial tension test using a materials testing system (Instron 3345) at a rate of 5 mm/s with a 0.2 N preload. Raw capacitance was measured using an LCR meter (E4980AL, Keysight Technologies). The sensors were loaded into the Instron such that their initial gauge length was the distance between the clamps. Strain limiting tabs were placed on either end of the sensors to prevent strain where the grips of the Instron

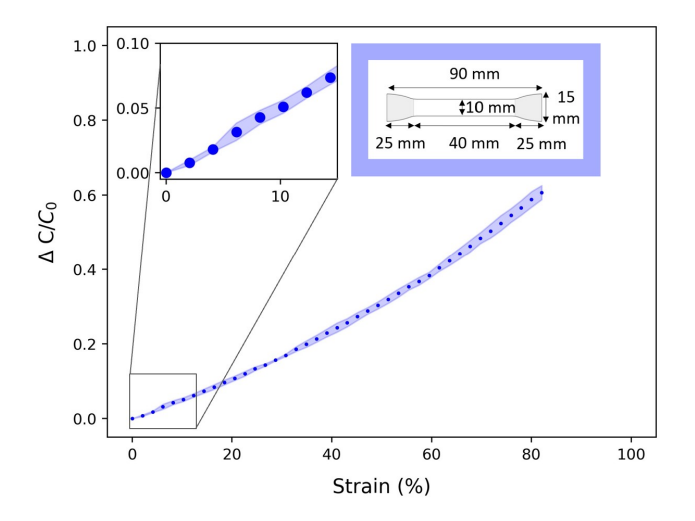


Fig. 2. Average normalized change in capacitance vs. strain for five fabric sensors. The capacitance of the sensors was recorded using the materials testing system (Instron 3345) and an LCR meter (E4980AL, Keysight Technologies) at an excitation frequency of 1 kHz.

clamped the sensors (shaded regions in Figure 2 inset). Five sensors were pre-stretched to 100% of their initial gauge length 10 times each before testing to account for the plastic deformation resulting from the initial strain [25].

Figure 2 shows the free space electromechanical characterization of the unit sensors. The dimensions of the sensor are shown in the top right inset. The shaded regions of the sensor schematic represent strain-limiting tabs while the remaining portion of the sensor is the gauge area. The vertical axis shows capacitance values normalized with respect to the capacitance of the gauge of each sensor since the strain limiting tabs did not stretch throughout the duration of the uniaxial tension test. The lower strain region ($\varepsilon < 10\%$) is highlighted in the top left corner of the graphic. This regime shows the expected operation region of the sensors resulting from the small displacements they will experience on the hand. The blue line demonstrates the normalized change in capacitance as a function of strain for the sensor with an error cloud representing the standard deviation of five samples. Elastomer-based capacitive strain sensors [26] exhibit a linear signal response because the dielectric elastomer is an isotropic material. In contrast, the sensors in this work have a nonlinear signal response due to the fabrics' anisotropy and inherent changes in the fabric's mesostructure during deformation [27]–[29].

Following free space characterization, further characterization to evaluate the effects of on-hand boundary conditions was performed. In contrast to the previous free-space characterization, strain in the on-hand characterization was attributed to joint bending and the associated pressure points. As such, change in capacitance with respect to joint bend angle was measured rather than strain. Using the fabrication process previously described, a sample glove was fabricated with sensors only spanning the pointer finger and thumb. The pointer and thumb were selected because it is assumed that the motion of the pointer finger is representative of the

middle, ring, and pinky fingers, while the motion of the thumb is unique. Strain limiting tabs were placed to outline the gauge length of the sensors, as done in the free space characterization. The integrated sensors were pre-stretched to 100% strain 10 times to expose the sensors to the same amount of plastic deformation as the free space sensors.

During data collection, the joint being characterized was moved into the frame of the motion capture system (PhaseSpace, Inc.) at a neutral horizontal (zero-degree) position. The respective joint was bent to the maximum range achievable, held for three seconds, and then returned to the neutral horizontal position. Capacitance was measured with a commercial capacitive sensing breakout board (MPR121; Adafruit) and an Arduino Uno, and the capacitance measurements were synchronized with the motion capture measurements using the Robot Operating System (ROS).

The four subplots in Figure 3 relate the normalized change in capacitance to joint bending angle (θ) for four different joints. The top row shows the relationship between the bending angle (θ) and normalized change in capacitance for the PIP joints of the thumb (in red) and pointer finger (in blue) while the bottom row represents the same relationship for the MCP joints. In these bound-unit characterizations, the sensors are subjected to pressure effects in addition to axial strain, introducing additional nonlinearities and giving the curves a different shape than the free space experiments. This phenomenon is especially apparent in the sensors on PIP joints, which are subjected to greater compression from bending over the PIP joint and fingertip [30]. The PIP joints are also subjected to larger ranges of θ than the MCP joints.

In general, the change in capacitance imposed by the PIP and MCP joints is much smaller than the change in capacitance observed in free space. A comparison between

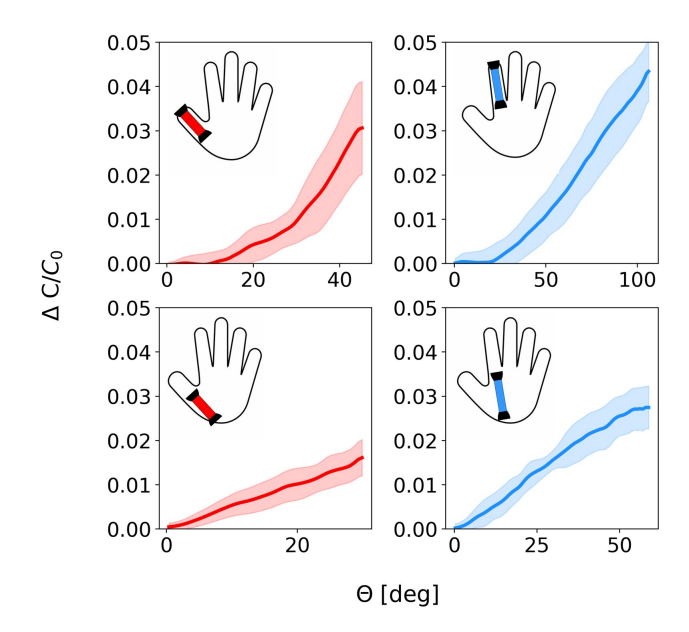


Fig. 3. Average normalized change in capacitance vs. bending angles of the PIP (top) and MCP joints (bottom) of the thumb (red) and the pointer finger (blue). Error cloud represents one standard deviation.

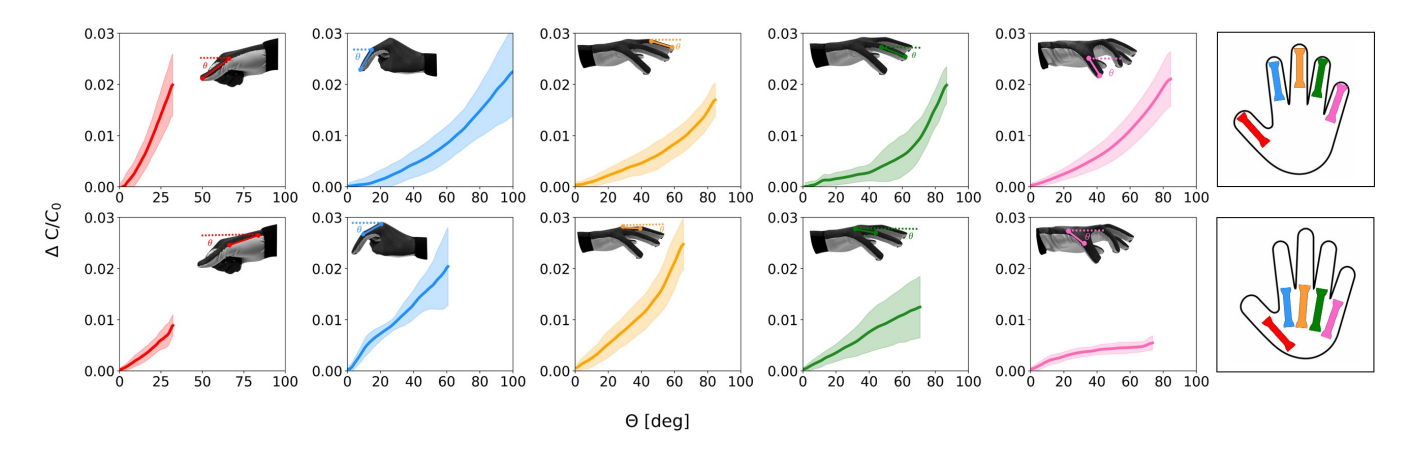


Fig. 4. Calibration of average relative change in capacitance vs. bending angles of the PIP (top row) and MCP joints (bottom row) of the thumb shown in red, index finger shown in blue, middle finger shown in yellow, ring finger shown in green, and pinky finger shown in pink. The insets depict the reference axis (zero-degree axis) defined for each joint bending angle to serve as ground truth.

the observed normalized change in capacitance with respect to bending angle (θ) can be mapped to strain in the regime of 0-10% in Figure 2.

IV. SYSTEM CHARACTERIZATION

To map the corresponding change in capacitance of each sensor to joint bend angle for the fully fabricated glove, data correlating these metrics were obtained. The same data collection process discussed above using motion capture was replicated for the fully fabricated glove system to calibrate the relationship between capacitance and ground truth joint angles from the motion capture system. Six trials were taken for each respective joint with the glove being removed and re-worn between trials to account for variations caused by the shifting placement of the glove expected in a practical application. Following the completion of the data trials, angle data representing the flexion of the joints from the neutral axis were extracted and aligned with the capacitance data. The final calibration curve for each sensor on each joint is presented in Figure 4, where the markers represent the mean and the error cloud represents the standard deviation. The xaxis of each subplot refers to the angle defined in each inset diagram.

TABLE I
ERROR BETWEEN MEASURED AND ACTUAL JOINT ANGLES

Finger	Joint	Mean Error (degrees)	Standard Deviation (degrees)
Pointer	MCP	5.399	4.326
	PIP	8.794	7.574
Middle	MCP	4.498	3.742
	PIP	9.486	5.679
Ring	MCP	5.045	4.378
	PIP	5.010	4.237
Pinky	MCP	7.972	7.250
	PIP	7.359	4.715
Thumb	MCP	3.096	2.352
	PIP	5.305	3.294

The pressure effects can be observed in the sensor response in Figure 4, especially for the PIP joints, which is congruent with the bound-unit characterization results shown in Figure 3. Overall, the PIP joint data are similar in both magnitude and trend. The MCP joint data are shown in the bottom row of Figure 4. The MCP joint of the middle finger has the most prominent protrusion and curvature when flexed, so there is a greater pressure imposed on that sensor at higher bend angles, resulting in a more sharply increasing capacitance value at higher angles. There is a tapering effect for the MCP joint of the pinky at higher joint angles. The pinky MCP joint protrudes the least of any joint on the glove. Therefore, it is not surprising that the resulting change in capacitance is relatively low with a small range.

Following the calibration of the system shown in Figure 4, further experimentation was performed to determine the accuracy of the glove. Data was acquired to obtain ground truth joint bend angle and a measured joint bend angle was calculated from the capacitance value recorded during motion. These calculated angles were compared to the ground truth angle measurement to assess the accuracy of the glove. Similar to previous modes of data acquisition, a motion capture system (PhaseSpace, Inc.) was used to take another data trial for each joint. The mode of data collection remained the same as the calibration step except that there was no extended hold at the maximum flexion point; instead, there was a constant motion between the zero and maximum joint bend angle. The resulting capacitance measurements were then used to predict the joint angle compared to the ground truth angle from the motion capture system. A nearest-neighbor interpolation model was applied using each of the calibration curves outlined in Figure 4 as the known relation to calculate the measured angle directly from capacitance. The resulting mean error and standard deviation between the measured and ground truth angles are reported for each joint in Table I. The thumb MCP joint demonstrates the lowest mean error (3.096 degrees) while the middle PIP joint has the highest mean error (9.486 degrees).

Figure 5 shows the resulting ground truth versus measured

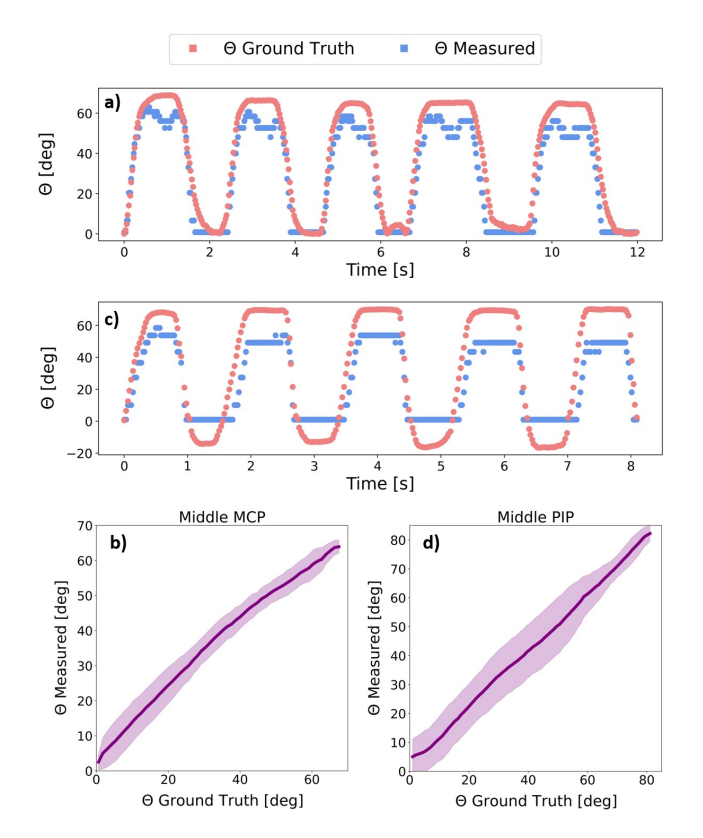


Fig. 5. Plots of ground truth and measured pose angles for (a-b) middle MCP joint, and (c-d) middle PIP joint.

angles for the joints with the highest (middle PIP) and second-lowest (middle MCP) reported mean errors. Although the thumb MCP shows the lowest mean error, we plot the middle MCP joint instead because it has a greater range of motion. The ground truth and measured angles for the joints over five flexion cycles are shown as a function of time in seconds in Figure 5a,c while in Figure 5b,d the measured angle is plotted vs. ground truth angle (the error cloud shows the standard deviation). The one-to-one mapping between the measured and actual angles confirms the accuracy and utility of the sensors in our glove application.

Figure 5a,c shows that the model is under-predicting the maximum value of θ at the peak and is most accurate during dynamic motions, which could be an effect of small amounts of noise present in the sensor when held at a constant value. Further, the calibration step did not account for angles above the defined neutral axis, and thus any motion corresponding to a negative θ is not accurately estimated. We suspect that such negative θ values resulted from the hand not being held directly perpendicular to the plane in which the analysis was performed or from joint hyperextension. Future work will aim to include these more complex motions with extended calibration. Finally, we note that the timescale of the data taken for the MCP joint is slightly longer than that of the PIP joint, which points toward future work regarding the effect of rate on accuracy and sensitivity.

V. Demonstration

Following the quantification of the accuracy of the glove, we sought to visually present the joint bend angles directly from the glove's capacitance readings. To demonstrate the accuracy and utility of the fabric sensor glove, we dynamically reconstructed the pose of a hand in Euclidean free space. The corresponding segmented images from the real-time reconstruction of the moving hand are shown in Figure 6. A demonstration of varying gestures was invoked through the use of American Sign Language spelling out "YALE." The top row shows the actual position of the hand while the bottom row shows the reconstruction of the hand with the intended letter from the capacitance values recorded from each sensor during motion. Figure 6 shows similar matching between the intended position and the reconstruction. Throughout each gesture, the thumb is the most inconsistent when compared to the actual form factor of the hand. Due to the number of degrees of freedom of the thumb and its complex motions, this is an expected result. While this work only characterized the motion of the thumb with respect to a single plane, it paves the way for greater data acquisition yielding more advanced reconstructions in the future.

VI. CONCLUSION

With this research, we sought to fabricate, calibrate, and quantify the accuracy of a fabric sensing glove. The fabrication demonstrated an array of ten capacitive fabric sensors with minimal infrastructure, such that the full natural motion of the hand remains intact. Free-space characterization demonstrates the electromechanical response with respect to uniaxial strain. Bound-unit characterizations performed on the hand for the pointer finger and thumb demonstrated the effects of coupled strain and localized pressure points when the sensor is applied to finger joints. The PIP and MCP joint sensors exhibited monotonic, nonlinear signal responses. Onhand calibration of the whole glove shows a repeatable and recognizable change in capacitance with respect to joint bend angle for all joints. Overall, the system demonstrates the ability to reconstruct joint bend angles with a root mean square error of 7.2 degrees. Finally, the glove was used to reconstruct dynamic hand poses in American Sign Language using the output capacitance values from the sensors.

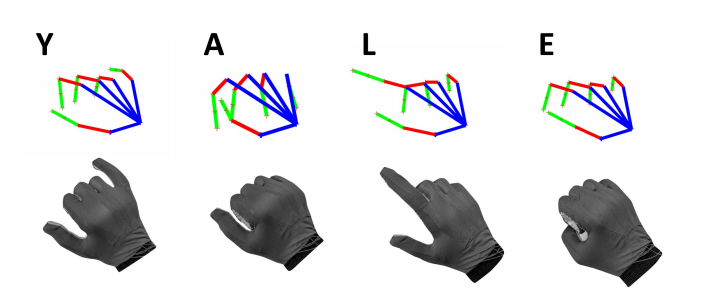


Fig. 6. Pose reconstruction (top row) and corresponding photographs depicting the intended hand positions for the letters spelling the word "Yale" in American Sign Language (ASL) (bottom row).

This work has demonstrated the dynamic reconstruction of the PIP and MCP joints of the hand using a fabric sensing glove. Future work aims to improve the calibration by including a broader range of motions, accounting for hyperextensions and more degrees of freedom. The unique motion of the thumb requires further characterization in multiple planes for accurate reconstruction of its complex movements. Furthermore, the development of this technology at multiple scales to account for a range of hand forms and sizes may call for further characterization beyond the scope of what is presented here. Leveraging machine learning algorithms would aid in increasing the robustness of the system from a modeling perspective. We have demonstrated a form-fitting, lightweight, and comfortable sensing glove that accurately and dynamically monitors human hand motion toward VR applications and gesture-controlled robots.

ACKNOWLEDGMENT

This research was funded by the National Science Foundation through IIS under grant no. IIS-1954591. We thank Dr. Huanbo Sun for helpful discussions.

REFERENCES

- S. S. Mechael, Y. Wu, Y. Chen, and T. B. Carmichael, "Ready-to-wear strain sensing gloves for human motion sensing," *Iscience*, vol. 24, no. 6, p. 102525, 2021.
- [2] P. Kumari, L. Mathew, and P. Syal, "Increasing trend of wearables and multimodal interface for human activity monitoring: A review," *Biosensors and Bioelectronics*, vol. 90, pp. 298–307, 2017.
- [3] W. Wang, R. Li, Z. M. Diekel, Y. Chen, Z. Zhang, and Y. Jia, "Controlling object hand-over in human-robot collaboration via natural wearable sensing," *IEEE Transactions on Human-Machine Systems*, vol. 49, no. 1, pp. 59–71, 2018.
- [4] D. Kim, J. Kwon, S. Han, Y.-L. Park, and S. Jo, "Deep full-body motion network for a soft wearable motion sensing suit," *IEEE/ASME Transactions on Mechatronics*, vol. 24, no. 1, pp. 56–66, 2018.
- [5] Y. Mengüç, Y. L. Park, E. Martinez-Villalpando, P. Aubin, M. Zisook, L. Stirling, R. J. Wood, and C. J. Walsh, "Soft wearable motion sensing suit for lower limb biomechanics measurements," pp. 5309– 5316, 2013.
- [6] N. Afsarimanesh, A. Nag, S. Sarkar, G. S. Sabet, T. Han, and S. C. Mukhopadhyay, "A review on fabrication, characterization and implementation of wearable strain sensors," *Sensors and Actuators A: Physical*, vol. 315, p. 112355, 2020.
- [7] H. Souri, H. Banerjee, A. Jusufi, N. Radacsi, A. A. Stokes, I. Park, M. Sitti, and M. Amjadi, "Wearable and stretchable strain sensors: materials, sensing mechanisms, and applications," *Advanced Intelligent Systems*, vol. 2, no. 8, p. 2000039, 2020.
- [8] M. Caeiro-Rodríguez, I. Otero-González, F. A. Mikic-Fonte, and M. Llamas-Nistal, "A systematic review of commercial smart gloves: Current status and applications," Sensors, vol. 21, no. 8, p. 2667, 2021.
- [9] P. Weber, E. Rueckert, R. Calandra, J. Peters, and P. Beckerle, "A low-cost sensor glove with vibrotactile feedback and multiple finger joint and hand motion sensing for human-robot interaction," in 2016 25th IEEE International Symposium on Robot and Human Interactive Communication (RO-MAN), pp. 99–104, IEEE, 2016.
- [10] J. DelPreto, J. Hughes, M. D'Aria, M. de Fazio, and D. Rus, "A wear-able smart glove and its application of pose and gesture detection to sign language classification," *IEEE Robotics and Automation Letters*, vol. 7, no. 4, pp. 10589–10596, 2022.
- [11] J. Pan, Y. Luo, Y. Li, C.-K. Tham, C.-H. Heng, and A. V.-Y. Thean, "A wireless multi-channel capacitive sensor system for efficient glove-based gesture recognition with ai at the edge," *IEEE Transactions on Circuits and Systems II: Express Briefs*, vol. 67, no. 9, pp. 1624–1628, 2020.
- [12] A. Tognetti, N. Carbonaro, G. Zupone, and D. De Rossi, "Characterization of a novel data glove based on textile integrated sensors," in 2006 International Conference of the IEEE Engineering in Medicine and Biology Society, pp. 2510–2513, IEEE, 2006.

- [13] A. Atalay, V. Sanchez, O. Atalay, D. M. Vogt, F. Haufe, R. J. Wood, and C. J. Walsh, "Batch fabrication of customizable siliconetextile composite capacitive strain sensors for human motion tracking," Advanced Materials Technologies, vol. 2, no. 9, p. 1700136, 2017.
- [14] J. S. Heo, H. H. Shishavan, R. Soleymanpour, J. Kim, and I. Kim, "Textile-based stretchable and flexible glove sensor for monitoring upper extremity prosthesis functions," *IEEE Sensors Journal*, vol. 20, no. 4, pp. 1754–1760, 2019.
- [15] S. Kim, D. Jeong, J. Oh, W. Park, and J. Bae, "A novel all-in-one manufacturing process for a soft sensor system and its application to a soft sensing glove," in 2018 IEEE/RSJ International Conference on Intelligent Robots and Systems (IROS), pp. 7004–7009, IEEE, 2018.
- [16] B. G. Lee and S. M. Lee, "Smart wearable hand device for sign language interpretation system with sensors fusion," *IEEE Sensors Journal*, vol. 18, no. 3, pp. 1224–1232, 2017.
- [17] O. Glauser, S. Wu, D. Panozzo, O. Hilliges, and O. Sorkine-Hornung, "Interactive hand pose estimation using a stretch-sensing soft glove," ACM Transactions on Graphics (ToG), vol. 38, no. 4, pp. 1–15, 2019.
- [18] X. Hu, Y. Xu, H. Zhang, J. Xie, D. Niu, Z. Zhao, and X. Qu, "A survey on the fiber bragg grating (fbg) sensing glove," *IEEE Sensors Journal*, 2023.
- [19] J. C. McCaw, M. C. Yuen, and R. Kramer-Bottiglio, "Sensory glove for dynamic hand proprioception and tactile sensing," in *International Design Engineering Technical Conferences and Computers and In*formation in Engineering Conference, vol. 51760, p. V02BT03A025, American Society of Mechanical Engineers, 2018.
- [20] V. Sanchez, C. J. Walsh, and R. J. Wood, "Textile technology for soft robotic and autonomous garments," *Advanced functional materials*, vol. 31, no. 6, p. 2008278, 2021.
- [21] I. I. Shuvo, A. Shah, and C. Dagdeviren, "Electronic textile sensors for decoding vital body signals: State-of-the-art review on characterizations and recommendations," *Advanced Intelligent Systems*, vol. 4, no. 4, p. 2100223, 2022.
- [22] J. S. Heo, J. Eom, Y.-H. Kim, and S. K. Park, "Recent progress of textile-based wearable electronics: a comprehensive review of materials, devices, and applications," *Small*, vol. 14, no. 3, p. 1703034, 2018.
- [23] L. Sanchez-Botero, A. Agrawala, and R. Kramer-Bottiglio, "Stretchable, breathable, and washable fabric sensor for human motion monitoring," *Advanced Materials Technologies*, p. 2300378, 2023.
- [24] G. Bain, N. Polites, B. Higgs, R. Heptinstall, and A. McGrath, "The functional range of motion of the finger joints," *Journal of Hand Surgery (European Volume)*, vol. 40, no. 4, pp. 406–411, 2015.
- [25] S. Merabia, P. Sotta, and D. R. Long, "Unique plastic and recovery behavior of nanofilled elastomers and thermoplastic elastomers (payne and mullins effects)," *Journal of Polymer Science Part B: Polymer Physics*, vol. 48, no. 13, pp. 1495–1508, 2010.
- [26] W. R. Johnson, A. Agrawala, X. Huang, J. Booth, and R. Kramer-Bottiglio, "Sensor tendons for soft robot shape estimation," in 2022 IEEE Sensors, pp. 1–4, IEEE, 2022.
- [27] L. Sanchez-Botero, A. Agrawala, and R. Kramer-Bottiglio, "Stretchable, breathable, and washable fabric sensor for human motion monitoring," *Manuscript submitted for publication*, 2023.
- [28] V. Kumar, V. R. Sampath, and C. Prakash, "Investigation of stretch on air permeability of knitted fabrics part ii: effect of fabric structure," *Journal of the Textile Institute*, vol. 107, pp. 1213–1222, 10 2016.
- [29] G. Dusserre, L. Balea, and G. Bernhart, "Elastic properties prediction of a knitted composite with inlaid yarns subjected to stretching: A coupled semi-analytical model," *Composites Part A: Applied Science* and Manufacturing, vol. 64, pp. 185–193, 2014.
- [30] R. K. Kramer, C. Majidi, R. Sahai, and R. J. Wood, "Soft curvature sensors for joint angle proprioception," in 2011 IEEE/RSJ International Conference on Intelligent Robots and Systems, pp. 1919–1926, IEEE, 2011.